JCTC Journal of Chemical Theory and Computation

Article

pubs.acs.org/JCTC

Efficient Modeling of NMR Parameters in Carbon Nanosystems

Teobald Kupka,*[,†] Michał Stachów,[†] Elżbieta Chełmecka,[§] Karol Pasterny,[∥] Magdalena Stobińska,[⊥,#] Leszek Stobiński,[▽] and Jakub Kaminský[○]

[†]University of Opole, Faculty of Chemistry, 48, Oleska Street, 45-052 Opole, Poland

[§]Division of Statistics, Department of Instrumental Analysis, Medical University of Silesia, 30 Ostrogórska Street, 41-200 Sosnowiec, Poland

[∥]A. Chełkowski Institute of Physics, University of Silesia, 4 Uniwersytecka Street, 40-007 Katowice, Poland

[⊥]Institute of Theoretical Physics and Astrophysics, University of Gdańsk, 57 Wita Stwosza Street, 80-952 Gdańsk, Poland

[#]Institute of Physics, Polish Academy of Sciences, 32/46, al. Lotników, 02-668 Warsaw, Poland

[▽]Institute of Physical Chemistry, Polish Academy of Sciences, 44/52 Kasprzaka Street, 01-224 Warsaw, Poland

[○]Institute of Organic Chemistry and Biochemistry, Czech Academy of Sciences, Flemingovo Nam. 2., 166 10 Prague, Czech Republic

Supporting Information

ABSTRACT: Rapid growth of nanoscience and nanotechnology requires new and more powerful modeling tools. Efficient theoretical modeling of large molecular systems at the *ab initio* and Density Functional Theory (DFT) levels of theory depends critically on the size and completeness of the basis set used. The recently designed variants of STO-3G basis set (STO-3G$_{el}$, STO-3G$_{mag}$), modified to correctly predict electronic and magnetic properties were tested on simple models of pristine and functionalized carbon nanotube (CNT) systems and fullerenes using the B3LYP and VSXC density functionals. Predicted geometries, vibrational properties, and HOMO/LUMO gaps of the model systems, calculated with typical 6-31G* and modified STO-3G basis sets, were comparable. The ^{13}C nuclear isotropic shieldings, calculated with STO-3G$_{mag}$ and Jensen's polarization consistent pcS-2 basis sets, were also identical. The STO-3G$_{mag}$ basis sets, being half the size of the latter one, are promising alternative for studying ^{13}C nuclear magnetic shieldings in larger size CNTs and fullerenes.

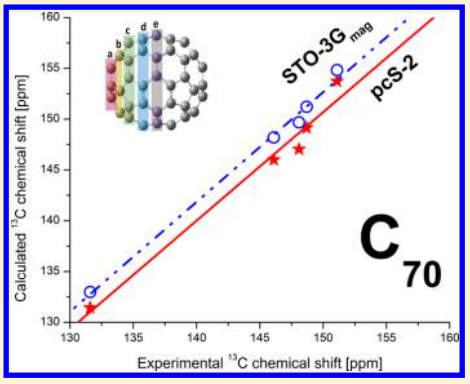

INTRODUCTION

The discovery of ordered carbon nanomaterials, including nanotubes (CNT[1−3]), fullerenes,[4] and graphene,[5] opened a new chapter in basic and applied research.[6−8] Due to their exceptional and unique chemical, mechanical and electronic properties,[9,10] the single- and multiple-wall CNTs (SWCNT and MWCNT) become promising elements in material science, electronics, spintronics, and medicine. They allow for examining quantum phenomena in single electron CNT quantum dots[11] or spin ordering and interaction in ^{13}C enriched CNT quantum dots.[12−14] Encapsulation of molecules in CNT was extensively studied toward high energy storage and its controllable release.[15] Some CNTs possess' ultra-high thermal stability and high tensile strength of CNTs led to production of high temperature resistant fibers. Besides, the electrical conductivity of outer layer of MWCNTs (ca. 3 orders of magnitude higher than Cu) indicates the possibility of their use in microchips and integrated circuits.[16] The very high porosity of these materials and large specific surface area[17] (from 100 to over 1000 m^2/g for CNTs comparing to ∼500 m^2/g for activated carbon) makes them promising candidates in physical sorption of neutral gases.[18−20]

The main obstacle in wide application of CNTs is their heterogeneity and presence of large amounts of amorphous carbon and metal catalyst impurities.[6,7] Thus, a direct experimental characterization of carbon materials using microscopic, X-ray, and spectroscopic techniques is often difficult.[21−23] Raman scattering is very popular among spectroscopic studies of CNT materials.[6,21,22,24] It enables a direct determination of SWCNT diameter d (in nm) since this parameter is inversely proportional to the radial breathing mode (RBM, expressed in wavenumbers), observed in the corresponding Raman spectrum:[25]

$$\mathrm{RBM} = 227/d \quad (1)$$

The above formula is slightly modified for small diameter SWCNTs:[24]

$$\mathrm{RBM} = (227/d) + 15 \quad (2)$$

The NMR method is the most powerful analytical technique in studying various aspects of both low molecular weight

Received: April 5, 2013
Published: July 18, 2013

systems and complex soft and solid materials.[26−32] However, it is a very rarely used tool in the CNTs research due to the presence of metal and sample inhomogenity.[32−36]

With the advent of the rapid development of computational chemistry, the experimental studies of carbon materials benefit from theoretical modeling of simplified molecular systems.[7,35,37,38] Theoretical *ab initio* or DFT methods are nowadays commonly used in predicting energetic, structural, and spectroscopic properties of small and middle size molecules.[39−41] Obviously, the achieved accuracy of theoretical predictions depends on the level of calculations, and thus implicitly on the size of the molecular systems, and can even reach the chemical accuracy (thermochemical parameters of small molecules, ∼1 kcal/mol). With the increasing size of the studied systems, several approximations in theory are needed. The "golden standard" theoretical method at the coupled cluster with single, double, and perturbative triple excitations[42,43] (CCSD(T)) level needs to be reduced for even middle-sized systems and some computationally significantly cheaper approach (e.g., DFT) must be employed.[44−47] Apart from the chosen theoretical method, the size of a basis set and its completeness is also crucial for obtaining accurate and reliable results.[48−52] In practice, a compromise of theory level and basis set quality is necessary to predict parameters of the studied system.[41,49,52−57]

Several extensive theoretical studies on structure, spectroscopic, and energetic parameters of model CNTs have been reported until now.[33−35,58−60] Latil and co-workers[61] used a very crude approximation to obtain magnetic response of a carbon nanotube. Besley and co-workers[62] used a more advanced theory to compute NMR parameters of finite *zigzag* and armchair CNTs. However, their results, calculated at Hartree−Fock level combined with a minimal size basis set (STO-3G), were unable to account for correlation effects. Indeed, such calculations, relying on fortuitous error calculations, could not be considered reliable nowadays.

The first seminal DFT studies on NMR chemical shifts of finite models of pristine (9,0) *zigzag* SWCNTs reported Zurek and Autschbach.[33] They considered nanotubes capped with H-atoms and fullerene semispheres as tips. The chemical shifts of the tips were significantly larger than in the middle of the tube. Two years later a study from the same group compared chemical shifts obtained using finite models of CNT and periodic calculations;[34] both types of calculations produced essentially similar results. The same authors[35] performed also the periodic calculations of NMR shifts within gauge-including projector-augmented plane wave (GIPAW), introduced by Mauri and co-workers[63,64] could not be used to examine armchair (metallic) nanotubes due to lack of efficient modeling of Knight-shift. To directly compare chemical shifts obtained from finite (molecular) and periodic calculations, Zurek and Autschbach[34] suggested the use of benzene as secondary reference. They also observed a decrease of chemical shift upon enlarging the tube diameter. This phenomenon was also calculated using GIPAW approach by Mauri and co-workers[64]

Thus far, some of theoretical studies were already used to interpret experimentally observed solid-state ^{13}C NMR spectra of metallic and semiconducting CNTs.[32,36,65] The recent experimental state-of-the-art study on unraveling carbon chemical shifts in ^{13}C labeled and separated samples of SWCNTs were reported by Engtrakul and co-workers.[32] They confirmed experimentally the theoretically predicted by Zurek and Autschbach and Mauri dependence of SWCNT carbon chemical shift decrease upon enlarging the tube diameter.

Our previous studies concentrated on theoretical predictions of structural and NMR properties of systematically enlarged models of pristine and functionalized SWCNTs.[66−68] In order to obtain reliable NMR shieldings, we used the polarization-consistent pcS-*n* basis sets.[69] This basis set series was designed for accurate prediction of nuclear shieldings. However, due to the size issue, only the pcS-2 basis set was used to model chemical shifts in our previous works on SWCNTs.[66−68] This basis set was used in calculations of models containing up to 100 carbon atoms. It is worth mentioning that, in the case of several linear polyacenes (up to pentacene), the RMS deviations of ^{13}C chemical shifts calculated at the B3LYP/pcS-2 level from experimental values in solution were fairly small (∼1 ppm). However, upon further increasing the size of the model, the pcS-2 becomes impractical.

Recently, two new basis sets, derived from the classical STO-3G and modified for calculation of electronic (STO-3G$_{el}$) and magnetic (STO-3G$_{mag}$) properties, were designed by Leszczyński and co-workers.[70] The authors reported a good performance of the STO-3G$_{mag}$ basis set in prediction of ^{1}H chemical shifts in benzene, naphtahalene, anthracene, and several other derivatives of phenanthrene at both RHF and DFT levels in comparison to experimental data.[70] The idea of STO-3G$_{el}$ and STO-3G$_{mag}$ basis sets arises from an extension of standard STO-3G basis set by functions obtained from analytical first-order correction function. Determination of such correction function originates from the solution of nonhomogeneous Schrodinger equation with a property perturbation operator corresponding to either electric field or magnetic field perturbations. The first-order correction corresponding to the homogeneous Schrodinger equation is then obtained using the Green's function. The authors then provided an analytical expressions for the correction functions of first-order perturbation theory for STO-3G basis in electric field and magnetic field, respectively. More details about the basis set construction and Green's function approach can be found in refs 70−72. The authors claim that, in contrast to response functions obtained from London AO, Green's function approach allows improving the quality of wave function (due to the solution of nonhomogeneous SE) in regions of configurational space most considerable for molecular property. Basis functions needed for correct description of molecule in electric or magnetic field (polarization and diffuse function in standard approach) are retrieved as linear combination of atomic STO of strictly defined type and quantity. Note that the determination of such additional functions requires no extra optimization of orbital exponents and contraction coefficients. Thus, in concrete, $1s^{(1)}(\xi_1)$ orbitals are for example expanded by $3p(\xi_1*0.333)$ for electric field and $2p^{(0)}(\xi_1*0.5)$ for magnetic field case, respectively. We found the labeling of new basis sets as STO-3G$_{mag}$ (or STO-3G$_{el}$) in some respect misleading, because new basis sets contain, for example, for carbon atoms, $1s(\xi_1)$, $2s(\xi_2)$, $2p(\xi_2)$, $2p(0.5*\xi_1)$, $3p(0.67*\xi_2)$, $3s(0.67*\xi_2)$, and $3d(0.67*\xi_2)$ orbitals. Similar expansion can be found for the STO-3G$_{el}$ basis set. Thus, this is no longer the STO-3G ($1s(\xi_1)$, $2s(\xi_2)$, $2p(\xi_2)$) basis set. It is, in the sense of a quality, somewhere between double and triple-ζ quality. Note, that STO-3G$_{el}$ and STO-3G$_{mag}$ are 10% less expensive (regarding the number of basis functions) than the split-valence triple-ζ 6-311G** basis set. It is also important to realize that the range of applicability of these new basis sets to

property calculations depends on the form of the perturbation operator. In the original paper, authors worked on the operators $\hat{W}_z^{el}(r) = -r\cos\theta$ and $\hat{W}_x^{mag} = -(e\hbar/2mc)[R \times \nabla]_x$.

Yet despite everything aforementioned, it would be desirable to test the performance of these relatively small basis sets, for predicting structural and spectroscopic parameters of nanocarbon models (e.g., pristine and functionalized SWCNTs). The application of small basis sets could extend the size of the computationally tractable systems and speed up the calculations. This could be a crucial step in accurate modeling of larger carbon systems without a compromise in accuracy of the obtained results. Thus, the aim of this study is to assess the applicability of newly available STO-3G$_{mag}$ and STO-3G$_{el}$ basis sets for accurate prediction of C−C bond lengths, HOMO/LUMO energy gaps, RBM wavenumbers, and ^{13}C NMR chemical shifts in selected reference compounds and simple models of SWCNTs. The size of the largest used models is at the borderline of nano-dimensions, and some of them also include experimentally characterized fullerenes. Thus, the (4,0) *zigzag* SWCNT models considered in our study are of 0.34 nm diameter and 1.1 nm length, and the C_{60} to C_{76} fullerene dimensions are about 0.7−0.9 nm.

COMPUTATIONAL METHODS

Geometry optimizations, vibrational analyses, and GIAO NMR[73,74] calculations of isotropic nuclear shieldings were performed in Gaussian 09 program.[75] A popular Becke three-parameter Lee−Yang−Parr exchange-correlation functional B3LYP was selected.[45,76] Additionally, the VSXC density functional was tested.[77] This functional was shown recently to produce fairly good NMR shieldings.[51] The geometry optimizations were performed using the unrestricted wave function aproximation with the very fine integration grid (GRID = 150590).

Benzene, phenol, aniline, and benzoic acid were selected as reference molecules used for testing theoretical approximations in reproducing experimental data (atom labeling in Scheme S1 in the Supporting Information). Structural fragments of these molecules resemble rims of pristine and −OH, NH_2, and COOH tip-functionalized SWCNTs. We were interested in bond lengths, HOMO−LUMO energy gaps, selected vibrational modes, and isotropic nuclear magnetic shieldings (recalculated to chemical shifts). In addition, the size of computational burden, expressed by a number of individual basis set functions N and CPU time were also part of the analysis.

The unrestricted B3LYP and VSXC calculations with the STO-3G, 3-21G, and 6-31G* basis sets were performed on series of simple model molecules with systematically increasing size.[66,68] The studied models included several linear acenes, cyclacenes, and *zigzag* (4,0) SWCNT fragments with terminal carbon atoms capped with hydrogen or a substituent (R = −H, −OH, $-NH_2$, and −COOH). These structures are depicted in Schemes 1−3. Bond labeling and arbitrary names of the model systems are also presented. Recently available STO-3G$_{el}$ and STO-3G$_{mag}$ basis sets were applied, and the results were critically evaluated. The largest studied molecules were nonacene with length of 2.2 nm, cyclacene (n = 8, diameter of 0.63 nm), and (4,0) *zigzag* SWCNT, formed from 5 basic units (0.34 nm diameter and length of 1.1 nm). Finally, we modeled fullerenes C_{60}, C_{70}, and C_{76} with a size ranging from 0.7 to 0.9 nm as examples of nano-objects, well characterized experimentally.

Scheme 1. Bond Labeling in Linearly Conjugated Planar (p) Benzene Rings (acenes, n = 1−9)

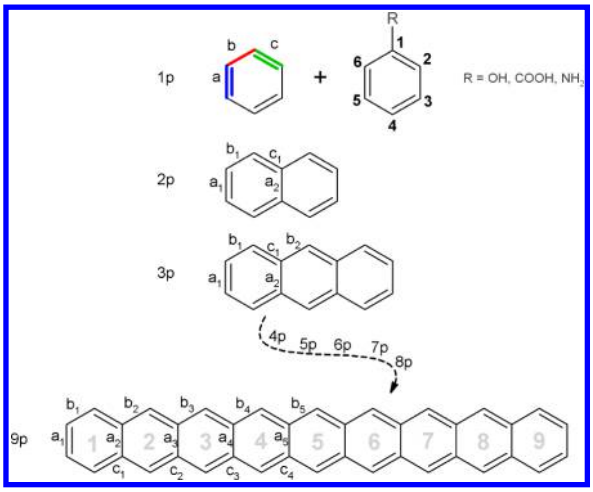

Scheme 2. Bond Labeling in Molecular "Belt" Systems (Cyclacenes, where n = 4−8)

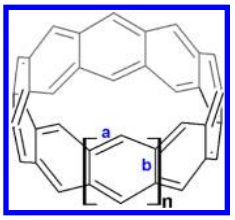

Experimental benzene bond lengths are taken from ref 78, and vibrational frequencies were from refs 79−82. The experimental MW structure of phenol was reported in refs 83−85, and vibrational data were taken from refs 84−88. The aniline experimental geometry was taken from refs 89 and 90, and vibrational data were from refs 89, 91, and 92. The experimental structure of benzoic acid was taken from refs 93 and 94, and vibrational numbers were from refs 95−100. Experimental C−C bond lengths in naphthalene,[101] anthracene,[101] tetracene,[102] and pentacene[103] are also available. However, to the best of our knowledge, no structural data for cyclacenes are available.

Extrapolation of selected C−C bond lengths, Raman RBM wavelengths, and ^{13}C nuclear shieldings and chemical shifts to the infinite system size (here number of benzene rings) was performed using a two-parameter formula:[53,68,104]

$$Y(x) = Y(\infty) + A/x^3 \quad (3)$$

where $Y(\infty)$ and A are the fitting parameters and x correspond to the size of a system. Here, $Y(\infty)$ is considered as a value of parameter Y for infinite size systems.

Chemical shifts of i-th carbon relative to TMS were obtained by using benzene as the secondary reference (see refs 66 and 67):

$$\delta_i = \sigma_{benzene} - \sigma_i + 128.5 \quad (4)$$

RESULTS AND DISCUSSION

1. Bond Lengths, Vibrations, and ^{13}C Nuclear Shieldings in the Reference Set. As a first part of our study, we checked the performance of modified STO-3G basis sets in predicting selected structural parameters, vibrational

dx.doi.org/10.1021/ct4002812 | J. Chem. Theory Comput. 2013, 9, 4275−4286

Scheme 3. Bond and Atom Labeling in Short *Zigzag* (4,0) SWCNT Model Consisting of Five "Bamboo" Units[a]

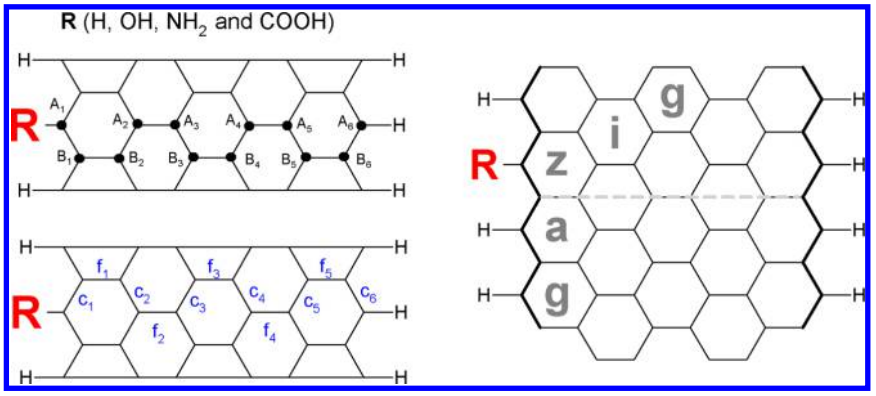

[a]A dashed line indicates tube axis and the two *zigzag* type rims are marked by a thicker line.

Table 1. Performance[a,b] of STO-3G$_{el}$ and STO-3G$_{mag}$ Basis Sets in Predicting Deviations of Bond Lengths (in Å) and Selected IR/Raman Vibrations (in cm^{-1}) from Experimental Values of Benzene, Phenol, Aniline, and Benzoic Acid

	basis set				
method	STO-3G	6-31G*	STO-3G$_{el}$	STO-3G$_{mag}$	pcS-2
			Bond Length		
B3LYP	0.0269	0.0051	0.0043	0.0075	0.0091
VSXC	0.0298	0.0111	0.0039	0.0086	0.0055
			Harmonic Vibration		
B3LYP	265.73	111.79	91.29	146.27	124.85
VSXC	248.21	95.25	92.05	124.34	114.85

[a]RMS values from experimental values are given. [b]Results obtained with selected basis sets are given for comparison.

modes, and ^{13}C nuclear shieldings in the set of reference molecules. The obtained parameters were compared to reported experimental values. The performance of standard STO-3G basis set and two others, suitable for predicting reasonable structural (6-31G*) and NMR parameters (pcS-2) were also analyzed.

Table 3. CPU Time (min) of Benzene Calculations

	CPU Time			
basis set	N	opt.	freq.	NMR
		B3LYP (VSXC)		
STO-3G	36	3.8 (7.2)	8.9 (10.4)	1.1 (2.3)
6-31G*	102	7.6 (16.8)	33.5 (55.4)	5.2 (5.7)
STO-3G$_{el}$	126	6.6 (37.5)	80.2 (132.5)	9.2 (11.2)
STO-G$_{mag}$	126	7.3 (36.3)	70.0 (125.5)	7.9 (14.2)
pcS-2	282	29.5 (69.9)	190.3 (301.9)	50.2 (44.1)

In order to present the capability of basis sets designed for electric or magnetic properties in predicting even structural parameters, deviations of theoretical C−C and C−H bond lengths in benzene from experimental values are gathered in Table S1 (Supporting Information).[78] The better agreement with experimental bond lengths was observed with the B3LYP functional, but the deviation of VSXC is only slightly worse.

Table 2. Deviations of ^{1}H and ^{13}C benzene Isotropic Shielding Constants (ppm) from Empirical Values

	basis set						
method	STO-3G	6-31G*	STO-3G$_{el}$	STO-3G$_{mag}$	pcS-2	lit.[a]	emp.[b]
			Same Method/Basis Set for Geometry and NMR Calculations[c]				
				^{13}C			
B3LYP	59.317	8.699	−8.048	−17.812	−17.482	2.961	59.905
VSXC	64.547	18.283	5.424	−3.464	−0.803		
				^{1}H			
B3LYP	1.617	1.067	0.875	0.238	0.117	0.205	23.90
VSXC	1.899	1.085	0.962	0.091	−0.098		
			B3LYP/6-31G* Geometry[d]				
				^{13}C			
B3LYP	62.318	8.699	−8.196	−17.704	−19.295	2.961	59.905
VSXC	67.964	19.150	6.283	−2.104	−1.210		
				^{1}H			
B3LYP	1.833	1.067	0.926	0.303	−0.011	0.205	23.90
VSXC	2.146	1.542	1.069	0.242	−0.147		

[a]Nuclear shielding from ref 51. [b]CCSD(T)/pcS-2 nuclear shielding at experimental geometry, see ref 51. ZPV corrections from ref 51 and experimental ^{13}C NMR values from ref 105 and ^{1}H data from refs 106 and 107. [c]Geometry optimization and NMR calculations performed using identical method and basis set. [d]GIAO NMR calculations on B3LYP/6-31G* geometry. Data were calculated with modified STO-3G basis sets combined with B3LYP and VSXC density functionals from empirical values.[51] Both geometry optimization and NMR calculations were performed using identical methods and basis sets and using the B3LYP/6-31G* geometry. Results for several basis sets and literature values are given for comparison.

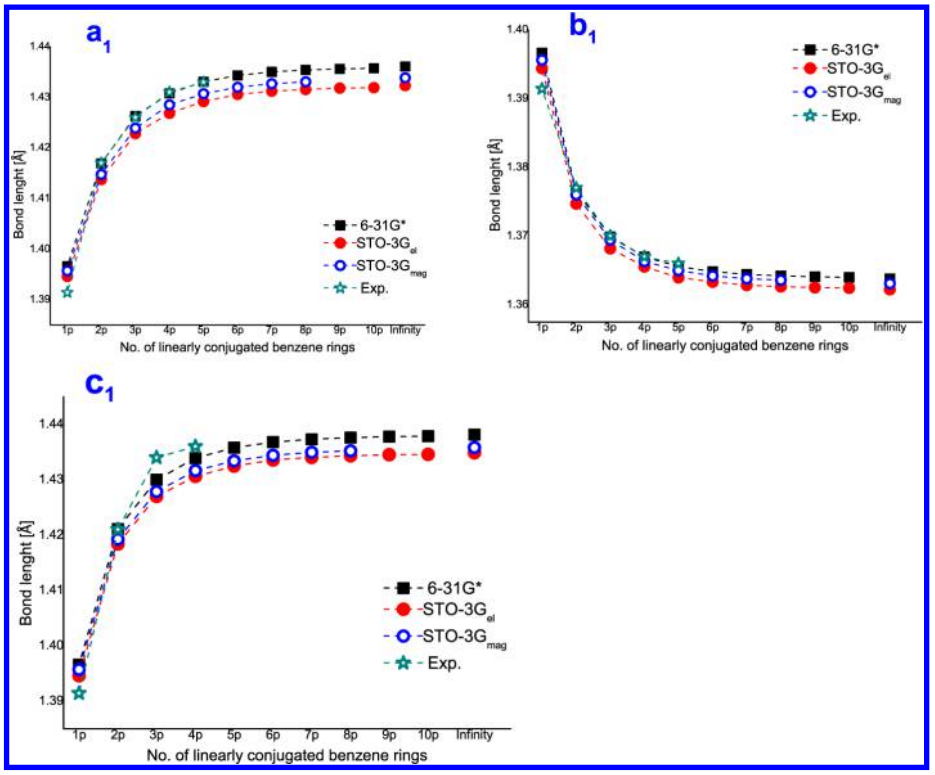

Figure 1. Regular convergence of three types of C−C bond lengths in polyaromatic hydrocarbons, calculated using B3LYP combined with 6-31G*, STO-3G$_{mag}$, and STO-3G$_{el}$ basis sets, upon increasing the number of linearly conjugated benzene rings (see Scheme 1): (A) a_1 type, (B) b_1 type, (C) c_1 type. Experimental data are from refs 78, 101−103 and individual points are connected for the reader's convenience.

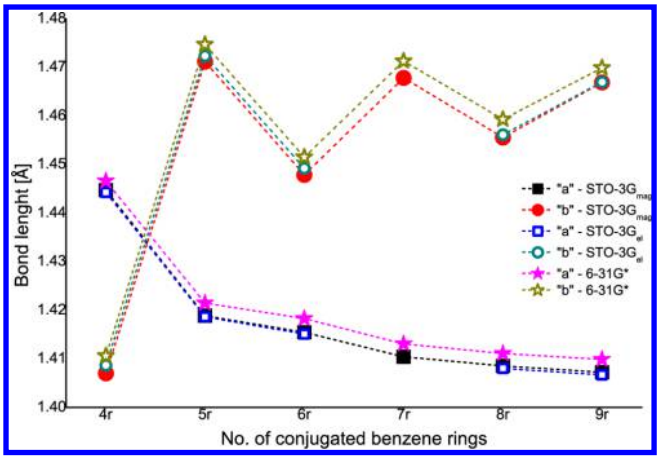

Figure 2. Convergence of two different types of C−C bond lengths (*a* and *b*, see Scheme 2) in cyclacenes calculated using B3LYP density functional combined with 6-31G*, STO-3G$_{mag}$, and STO-3G$_{el}$ basis sets upon increasing the number of benzene rings. In some cases, very similar results obtained with different basis set are indicated by overlapping marks. Individual points are connected for the reader's convenience.

The accuracy according to the basis set used decreases in the following order: pcS-2 > 6-31G* > STO-3G$_{el}$ > STO-3G$_{mag}$ > STO-3G. The STO-3G$_{el}$ and STO-3G$_{mag}$ basis sets perform fairly well and overestimate the C−H bond only by about 0.01 Å. A similar performance is observed for the C−C bond. Additionally, selected vibrational modes provided by STO-3G$_{el}$ and STO-3G$_{mag}$ are also listed in the Table S1 (Supporting Information). Both density functionals yield harmonic frequencies of similar accuracy (experimental values are

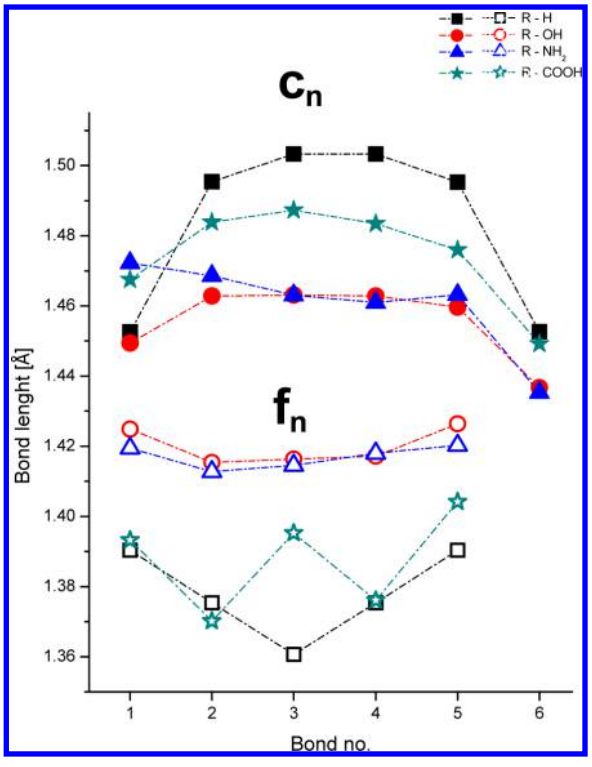

Figure 3. Influence of the tip-substituent nature on (A) c_1 to c_6 and (B) f_1 to f_5 type of C−C bond length along the axis of a model *zigzag* (4,0) SWCNT. The bond-lengths were calculated at the B3LYP/6-31G** level. In some cases, very similar results obtained for different functionalization are indicated by overlapping marks. For reader's convenience the individual points are connected.

dx.doi.org/10.1021/ct4002812 | J. Chem. Theory Comput. 2013, 9, 4275−4286

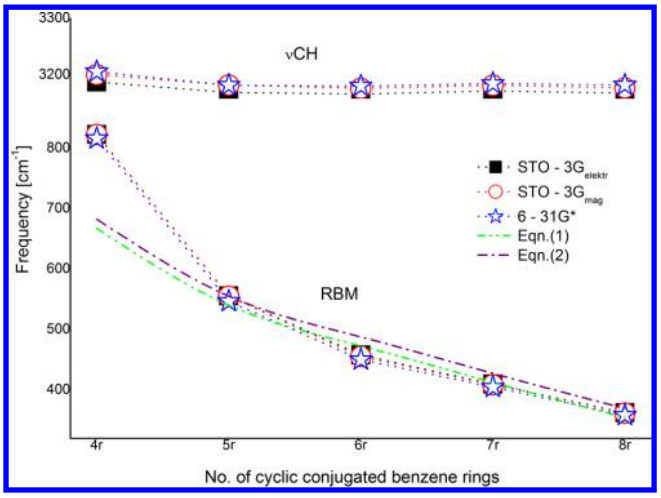

Figure 4. Convergence of RBM and ν(CH) wavelengths in cyclacenes upon increasing the number of benzene rings, calculated using B3LYP density functional combined with 6-31G*, STO-3G$_{mag}$, and STO-3G$_{el}$ basis sets. In some cases, very similar results obtained with different basis set are indicated by overlapping marks. Empirical results for SWCNTs calculated with eq 1 and 2 are shown for comparison. Individual points are connected for the reader's convenience.

overestimated up to 5% due to not taking anharmonicity into account). The standard STO-3G basis set performs significantly worse than its modified variants in predicting harmonic frequencies (higher by about 15%). In general, we can conclude that the STO-3G$_{el}$ basis set performs slightly better than STO-3G$_{mag}$ in predicting benzene bond lengths and harmonic frequencies. Similar results were observed for selected bond lengths and harmonic vibrational frequencies for phenol, aniline, and benzoic acid. Values are shown in Tables S2−S4 in the Supporting Information.

In general, the standard STO-3G basis set is very inaccurate in predicting bond lengths or vibrational modes. Both structural and vibrational parameters obtained with Leszczyński's STO-3G$_{el}$ and STO-3G$_{mag}$ basis sets are significantly more accurate and close to those obtained with 6-31G* basis set but less reliable than from significantly larger calculations using pcS-2. We could conclude the use of specific basis sets for magnetic or electric properties here do not deteriorate geometrical properties. The overall summary of bond lengths provided by several basis sets on small reference aromatic compounds are gathered in Table 1. Predictions of harmonic vibrations are presented as well.

In the next step, the accuracy of isotropic nuclear magnetic shieldings, predicted with the STO-3G$_{el}$ and STO-3G$_{mag}$ basis sets, was studied (Table 2). In this case, the geometry used in GIAO calculations is also an important issue, and it needs to be taken into account. Thus, first the same combination of method and basis set was used for the optimization and calculation of NMR properties. Next, assuming that B3LYP/6-31G* level of theory produces fairly accurate structure (as obvious from Table 1 and refs 54, 66−68), only NMR shielding calculations varied with respect to density functional type and basis set.

It is evident from the Table 2 that both carbon and proton shieldings in benzene calculated with the VSXC functional are significantly closer to experiment (precisely, to empirical data, e.g., experimental values including zero-point rovibrational corrections) than those, obtained with the B3LYP. Besides, the standard STO-3G basis set leads to an unacceptable overestimation of shieldings (carbons by 59 to 64 ppm, and protons by 1.6 to 1.9 ppm for VSXC and B3LYP). The Pople type basis set 6-31G* leads to significant deviations from experiment, too. The pcS-2 basis set designed for NMR shielding calculations produces results close to experiment.[105] However, it is very pleasing to observe that both carbon and proton nuclear shieldings in benzene, calculated with the STO-3G$_{mag}$ basis set, are close to values obtained with the significantly larger (and more expensive computationally) pcS-2 basis set. Thus, the best results obtained with new basis sets are observed for VSXC/STO-3G$_{mag}$ calculations (carbon and proton deviations are only about −3.5 and 0.1 ppm). The GIAO calculations performance is very similar when using the B3LYP/6-31G* geometry (only a small deterioration of accuracy is observed in Table 2). This

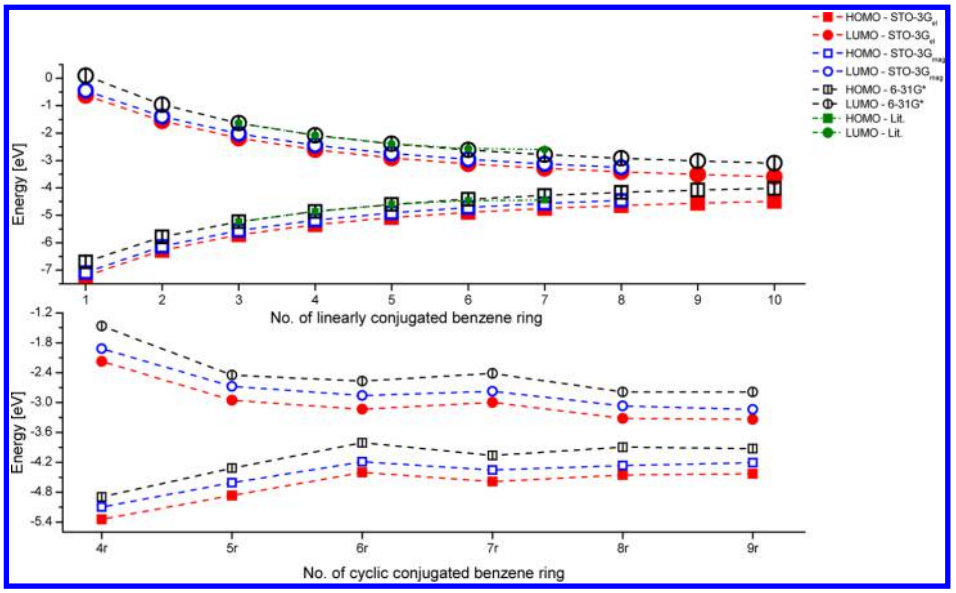

Figure 5. B3LYP calculated HOMO and LUMO molecular orbital energies [eV] in polyacenes (top) and cyclacenes (bottom) as a function of the number of benzene rings (n). In some cases, very similar results obtained with different basis set are indicated by overlapping marks. Individual points are connected for the reader's convenience.

dx.doi.org/10.1021/ct4002812 | J. Chem. Theory Comput. 2013, 9, 4275−4286

Table 4. B3LYP Calculated HOMO−LUMO Gap [eV] for Linear acenes, Cyclacenes, and *Zigzag* (4,0) SWCNT Containing 5 "Bamboo" Units

	HOMO−LUMO gap [eV]				
	basis set				
molecular system	6-31G*	STO-3G$_{el}$	STO-3G$_{mag}$	lit.	exp.
	Polyacene				
1p	6.8[a]	6.59[e]	6.64[e]		5.96[f]
2p	4.83[a]	4.73[e]	4.74[e]		4.45[g]
3p	3.59[a]	3.53[e]	3.53[e]	3.59[b]	3.45[g]
4p	2.78[a]	2.73[e]	2.73[e]	2.78[b]	2.72[g]
5p	2.21[a]	2.17[e]	2.16[e]	2.21[b]	2.31[g]
					2.29[g]
6p	1.8[a]	1.77[e]	1.75[e]	1.89[b]	1.90[g]
7p	1.49[a]	1.46[e]	1.44[e]	1.86[b]	1.35[h]
8p	1.25[a]	1.23[e]	1.20[e]		
9p	1.06[a]	1.05[e]			
infinity	0.91[a]			1.61	≈1.2[i]
infinity[c]	**0.77**[a]	**1.11**[e]	**1.28**[e]	**1.86**[e]	**1.55**[e]
	Cyclacene				
4r	3.43[a]	3.17[e]	3.18[e]		
5r	1.87[a]	1.91[e]	1.93[e]		
6r	1.24[a]	1.27[e]	1.33[e]		
7r	1.65[a]	1.59[e]	1.58[e]		
8r	1.11[a]	1.14[e]	1.20[e]		
infinity[d]	**1.09**[a]	**1.36**[e]	**1.38**[e]		
pristine (4,0) SWCNT (4r5u)	1.05[e]				
(4,0) HO-SWCNT (4r5u)	1.08[e]				
(4,0) H_2N-SWCNT (4r5u)	1.09[e]				
(4,0) HOOC-SWCNT (4r5u)	1.09[e]				
$C_{60}(I_h)$	2.89[e]				2.3[j]
$C_{70}(D_{5h})$	2.69[e]				
$C_{76}(D_2)$	1.97[e]				

[a]From ref 67. [b]From ref 109. [c]CBS fit with eq 3. [d]Data for 7r excluded from fitting with eq 4. [e]This work. [f]From ref 111. [g]From ref 115. [h]Simplest measured derivative from ref 116. [i]Extrapolated value from ref 116. [j]From ref 112. Data obtained from extrapolation to infinite size systems are also included.

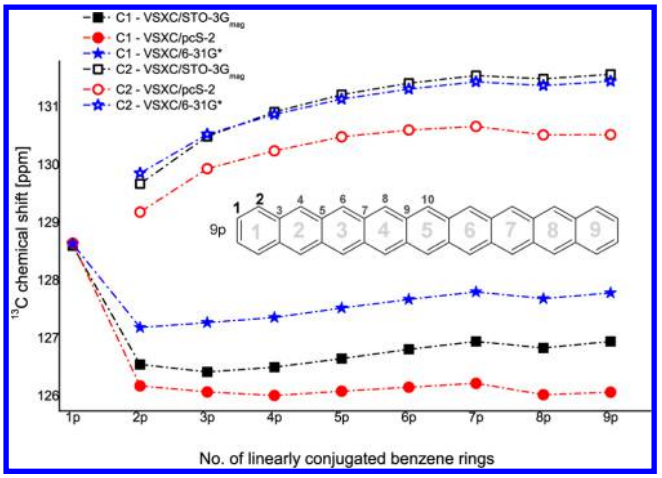

Figure 6. Different convergence of ^{13}C chemical shifts of two carbons (B3LYP/6-31G* geometry, C1 full marks, C2 empty marks) in polyaromatic hydrocarbons calculated with VSXC density functional combined with 6-31G*, STO-3G$_{mag}$, and pcS-2 basis sets, upon increasing the number of linearly conjugated benzene rings (see Scheme 1). In some cases, very similar results obtained with different basis set are indicated by overlapping marks. Individual points are connected for the reader's convenience.

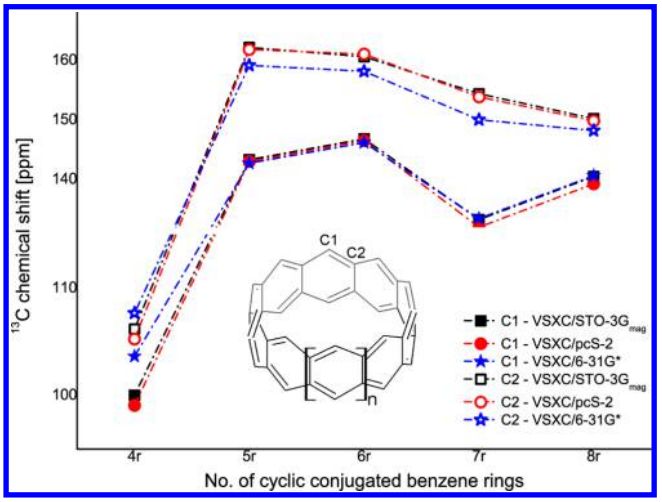

Figure 7. Different convergence of two types of ^{13}C chemical shifts in polyaromatic hydrocarbons (B3LYP/6-31G* geometry) calculated using VSXC density functional combined with 6-31G*, STO-3G$_{mag}$, and STO-3G$_{el}$ basis sets, upon increasing the number of benzene rings in cyclacenes (see Scheme 2). In some cases, very similar results obtained with different basis sets are indicated by overlapping marks. Individual points are connected for the reader's convenience.

supports our earlier studies—significantly better performance of the VSXC density functional in comparison to B3LYP in predicting accurate carbon shielding.[51]

Deviations of selected carbon shieldings from experimental values (all data taken from the SDBC database[108] and not corrected for ZPV) in phenol, aniline, and benzoic acid calculated with the B3LYP and VSXC density functionals and different basis sets are presented in Tables S5 and S6 in the Supporting Information. In Table S6a, the RMS deviations of selected calculated shieldings over all reference systems are shown. These results clearly show a good performance of the VSXC/STO-3G$_{mag}$ level in predicting isotropic shieldings within the whole reference test set.

The cost-to-performance aspect of calculations using modified basis sets is addressed in Table 3. Both the number of basis set functions and CPU time for geometry optimization, frequency, and GIAO NMR calculations for benzene are listed. All calculations were performed using 8 CPU units and 20 GB of RAM space. The size of STO-3G$_{el}$ and STO-3G$_{mag}$ basis sets is similar to 6-31G* and more than twice smaller than pcS-2. It is evident that B3LYP works significantly faster than VSXC in geometry optimization and frequency while for GIAO calculations the CPU times are nearly the same for both density functionals. Moreover, it is very encouraging that nuclear shieldings calculated using the VSXC density functional are about four times faster with the STO-3G$_{mag}$ basis set than with pcS-2.

2. Convergence with Size of Selected Parameters in Polyacenes (n = 1−9) and Cyclacenes (n = 4−8). Upon systematic increase of a number of benzene rings forming an acene, a regular change of structural parameters (e.g., C−C bond length) has been observed both experimentally and

dx.doi.org/10.1021/ct4002812 | J. Chem. Theory Comput. 2013, 9, 4275−4286

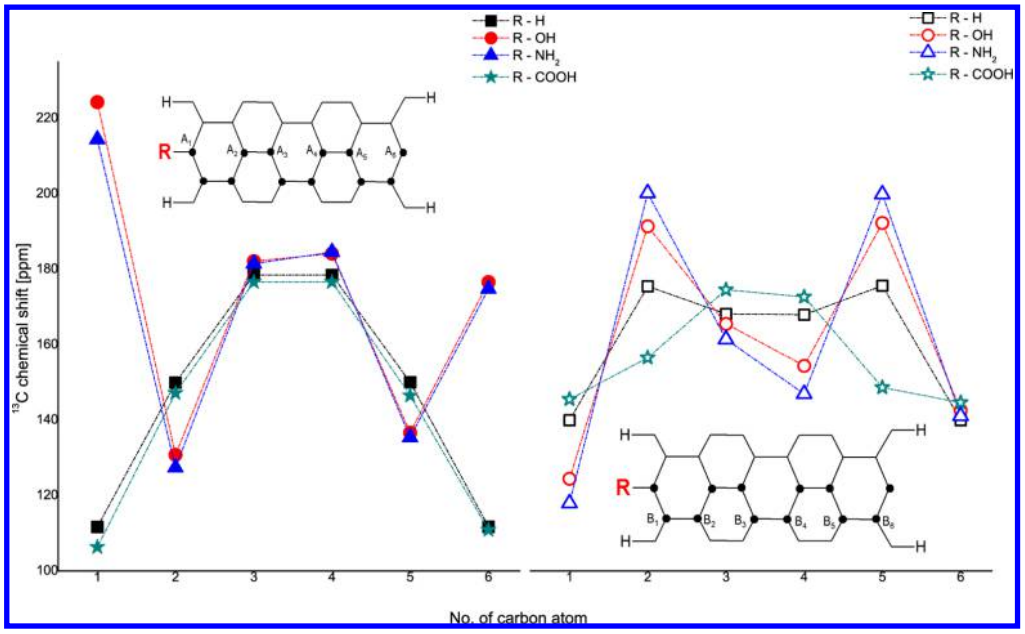

Figure 8. Different convergence of (A) A1 to A6 and (B) B1 to B6 types of ^{13}C chemical shifts in short functionalized *zigzag* (4,0) SWCNT along the tube axis (see Scheme 3). Structures were optimized with B3LYP/6-31G* method, and shifts were calculated using the VSXC density functional combined with STO-3G$_{mag}$ basis set. In some cases, very similar results obtained for different systems are indicated by overlapping marks. Individual points are connected for the reader's convenience.

theoretically (B3LYP/6-31G* results in refs 66, 67, 109, and 110). Changes of a_1, b_1, and c_1 bond lengths (see Scheme 1 for bond descriptions) calculated with B3LYP density functional and modified basis sets are shown in Figure 1. Data obtained with relatively large and well performing Pople type basis set 6-31G* are plotted, too, for comparison. A fairly good agreement is observed (within 0.005 Å) for benzene, naphthalene, anthracene, and pentacene comparing the calculated a_1 and b_1 bonds with experimentally observed values.[78,101−103,109,110] It is also evident that adding more than 6−7 benzene rings does not lead to any significant changes in C−C lengths and saturation is observed. Thus, it is reliable to estimate the limiting C−C bond lengths for an infinitely long acene using formula 3. Thus, the last points in plots of Figure 1 were obtained using the extrapolation formula 3. The results indicate that C−C bond lengths in acenes predicted with the B3LYP functional using STO-3G$_{el}$, STO-3G$_{mag}$, and 6-31G* basis sets are probably within experimental error bars (±0.005). The quality of prediction decreases in the row: 6-31G* > STO-3G$_{mag}$ > STO-3Gel (see Figure 1). Due to difficulties in experimental characteristic of longer acenes[71] only the first family members are compared with our theoretical predictions.

Two kinds of C−C bonds are distinguishable (*a* and *b*, see Scheme 2) in cyclacenes. The first type corresponds to intercarbon distances in a rim of *zigzag* SWCNTs. A convergence of *a* and *b* bonds in cyclacenes, calculated with B3LYP density functional, can be followed in Figure 2. The data show a roughly similar performance of the three basis sets (STO-3G$_{el}$, STO-3G$_{mag}$, and 6-31G*) used with the differences within ±0.005 Å. However, the convergence pattern is more complex and less regular for cyclacenes (see also refs 67 and 110) than it was with linear acenes. The length of bond *a* decreases roughly exponentially, on the other hand, the convergence pattern of the bond *b* resembles a damping curve (with decreasing oscillations). This kind of behavior has been observed earlier[67] in cyclacenes optimized at B3LYP/6-31G* level of theory.

3. Selected C−C Bonds in *Zigzag* (4,0) SWCNT. First we will consider changes of carbon−carbon bond lengths along a short *zigzag* (4,0) CNT made of five bamboo rings (units) starting from a functionalization place at the rim (for R = −H, −OH, −NH$_2$, and −COOH). These bonds are tilted by 60° relative to the tube axis and are arbitrary labeled c1 to c6 (see Scheme 3). In case of R = −H, a symmetrical shape is observed (Figure 3A) with short bonds at both rims (about 1.45 Å) and significantly longer in the middle of the tube (about 1.50 Å). An asymmetric pattern of C−C bond length changes is observed upon functionalization of CNT rim with one −OH, −NH$_2$, and −COOH substituent. In tip-mono functionalized CNT model the bond lengths close to both rims slightly differ. In addition, the bonds at the middle are significantly shortened. Interestingly, the presence of substituent with free electron pairs (−OH and −NH$_2$) have a very similar impact (shortening of C−C bonds in the middle of the tube by about 0.04 Å). The effect of −COOH substituent is two times smaller (shortening by about 0.02 Å). The C−C bonds parallel to CNT axis, labeled f_1 to f_5, are also sensitive to R−substituent type at the rim of CNT (Figure 3B). Comparing patterns in Figure 3A and B, an opposite effect is clearly visible: elongation of c-type bonds is accompanied with shortening of the corresponding f-type bond. As before, an impact of substituents with lone electron pairs is similar.

4. Cyclacenes RBM and ν(CH) Modes. The position of RBM in experimental Raman spectra of carbon nanotubes is an important spectroscopic feature enabling determination of their diameter.[6,24] Thus, it is worth comparing positions of the RBM band calculated at the B3LYP level using STO-3G$_{mag}$, STO-3G$_{el}$, and Pople's 6-31G* basis sets. The latter one was frequently used to calculate fairly accurate RBM mode in model SWCNTs.[66−68] A roughly exponential decreasing of the RBM frequency calculated with the B3LYP functional upon

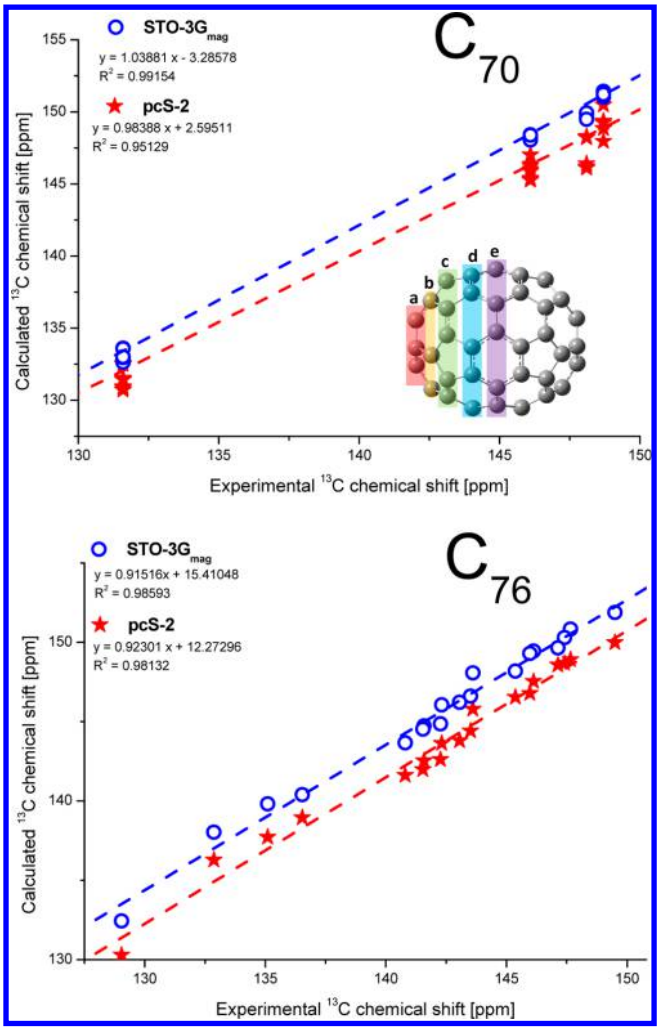

Figure 9. Performance of STO-3G$_{mag}$ and pcS-2 basis sets in predicting C_{70} (top) and C_{76} (bottom) ^{13}C NMR chemical shifts (in ppm) using VSXC density functional (B3LYP/6-31G* geometry).

increasing cyclacenes' diameters is shown in Figure 4. In fact, the results are very close for all three basis sets used (significantly overlapping marks). The similar pattern is observed for stretching ν(CH) mode. These data indicate a very similar behavior of the 6-31G*, STO-3G$_{mag}$, and STO-3G$_{el}$ basis sets in predicting cyclacenes vibrational modes. One could also assume similar results upon increasing SWCNT radius. Using eqs 1 and 2, we modeled changes of RBM in SWCNTs, characterized by the same diameter as the studied 4r to 8r cyclacenes. Indeed, a good agreement between empirically calculated RBM values of SWCNTs with eqs 1 and 2 and their very simplified models (e.g., cyclacenes) is apparent in Figure 4. It is interesting to notice that the DFT calculated value of RBM for the smallest r4 system is far off the empirical values, probably due to a very significant strain of its frame.

5. HOMO−LUMO Gaps in Linear Acenes and Cyclacenes. From a practical point of view, applications in electronic and optics require materials to have specific HOMO/LUMO gap features.[6,24,109−112] It is known that enlarging the aromatic system and allowing for more delocalized electron density leads to smaller energy gaps. Indeed, upon formation of longer polyacenes (Figure 5 top) a regular convergence of HOMO (from below) and LUMO (from above) orbital energy is observed leading to a decrease of energy gap to about 1 eV. Similar patterns are observed (Figure 5 bottom) for cyclacenes. It is important to mention that the HOMO and LUMO orbital energies predicted with 6-31G*, STO-3G$_{mag}$, and STO-3G$_{el}$ basis sets (all with the B3LYP functional) are within ±1 eV and the corresponding gaps within ±0.5 eV. In fact, the HOMO/LUMO energies and gap are close (Table 4) to earlier reported experimental values for several polyacenes.[67,109−111,113−116]

6. Selected ^{13}C NMR Chemical Shifts in Linear Acenes and Cyclacenes. In our previous study, we reported on ^{13}C NMR chemical shifts of linear acenes and their sensitivity toward the system size.[66] Indeed, some regular changes in chemical shifts of C1 and C2 atoms (see Scheme 1) upon enlarging acene systems are visible in Figure 6. Moreover, all the points, calculated with the B3LYP density functional and with 6-31G*, STO-3G$_{mag}$, and pcS-2 basis sets are close to each other (see partly overlapped marks for C2 and better separated for C1 chemical shifts calculated with pcS-2 and STO-3G$_{mag}$ basis sets). Each basis set seems to show a different sensitivity to the size of the system and the local electronic environment. Due to low quality, we can expect that the 6-31G* basis set produces the least reliable NMR results.

In cyclacenes, an initial increase and next a saturation of C1 and C2 chemical shifts changes, calculated with the B3LYP density functional and 6-31G*, STO-3G$_{mag}$, and STO-3G$_{el}$ basis sets, with their diameter is also observed (Figure 7). Moreover, both modified basis sets produce very similar numbers while 6-31G* basis set predicts values, different by about 10 ppm. Assuming that cyclacenes are very crude models of SWCNTs, we notice about 5−10 ppm decrease of C1 and C2 carbon chemical shifts upon enlarging their diameter from 0.38 to 0.64 nm (for n = 5 to n = 8). This trend agrees qualitatively with theoretically predicted changes in SWCNTs (see calculations by Zurek and Autschbach[34] and by Mauri[64]) and measurements by Engtrakul[32,117]).

7. Selected ^{13}C NMR Chemical Shifts in Zigzag (4,0) SWCNT. Next, carbon chemical shifts along a model *zigzag* (4,0) SWCNT, functionalized at the rim, were predicted using the VSXC density functionals and STO-3G$_{mag}$ basis set. An arbitrary atom labeling along the SWCNT axis was included in the graph (see also ref 66). First of all, an asymmetric profile of carbon chemical shifts along the tube axis is observed for A- and B-type carbon atoms in CNTs, monosubstituted at one end. This pattern resembles the behavior of C−C bond lengths with increasing system size shown previously in section 3. Obtained results indicate a saturation of carbon chemical shift values for atoms in the middle of CNT at about 180 ppm (Figure 8A and B). This very high value (and thus more deshielded carbons are calculated) is probably due to skeletal strain in the studied ultra-low diameter model. SWCNTs of such small diameter are not freestanding and exist in confined spaces only, for example, in multiwall CNTs or zeolite channels.[118] As before for bond lengths, energy gap, and vibrational properties, the results in Figure 8 also prove an excellent performance of STO-3G$_{mag}$ basis set in predicting ^{13}C NMR chemical shieldings in functionalized models of SWCNT.

8. ^{13}C NMR Chemical Shifts in C_{60}, C_{70} and C_{76} Fullerenes. The last part of our study was dedicated to the performance of STO-3G$_{mag}$ and pcS-2 basis sets in predicting ^{13}C chemical shifts of several fullerenes. Figure 9 shows linear correlation between experimental[117,119,120] and theoretical (the VSXC functional) ^{13}C NMR chemical shifts of C_{70} and C_{76} fullerenes. It is apparent that the STO-3G$_{mag}$ basis set being two times smaller than pcS-2 produces results of almost the same

quality. A closer inspection of chemical shift deviations between theory and experiment from several solution and solid state NMR experiments performed at C_{60}, C_{70}, and C_{76} is shown in Table S7 (Supporting Information). Our results indicate a fairly accurate prediction of fullerene carbon chemical shifts. Note that the corresponding RMS values depend on experiment, which the calculated data are compared with. Thus, the observed agreement is within a range of 1.3 (for pcS-2) and 3.3 ppm (for STO-3G_{mag}). These results additionally suggest using the modified basis set for practical and reasonable predictions of carbon NMR shifts. For example, in case of C_{76} system, the STO-3G_{mag} basis set means using of 1300 basis functions vs 2500 if pcS-2 is employed. Thus, obviously, the Leszczyński's basis sets enable predictions of accurate NMR parameters for significantly larger systems than it is possible with pcS-2 basis set.

CONCLUSIONS

Extensive DFT calculations using the B3LYP and VSXC density functionals and recently modified STO-3G_{el} and STO-3G_{mag} basis sets supported their potential use in theoretical works leading to predicting structural and NMR properties of model SWCNT systems. The models included benzene, acenes, cyclacenes, and short *zigzag* (4,0) SWCNTs before and after monosubstitution with −OH, $-NH_2$, and −COOH groups. In addition, phenol, aniline, and benzoic acid were tested as reference compounds, and their calculated parameters were compared with available experimental data. The STO-3G_{el} and STO-3G_{mag} basis sets were derived from a very small standard STO-3G basis set, which is completely excluded from current *ab initio* studies. The STO-3G_{el} and STO-3G_{mag} basis sets produced fairly accurate geometrical parameters, HOMO−LUMO energies and Raman RBM wavenumbers. We proved that even if the newly derived basis sets are about two times smaller than pcS-2 they allowed for very similar performance in case of NMR calculations. Thus, the NMR shieldings (and chemical shifts) of model SWCNTs were calculated significantly faster with STO-3G_{mag} basis sets without deterioration of accuracy as it happened with, for example, 6-31G*. The other advantage in using STO-3G_{mag} basis sets resulted from a possibility of increasing the size of tractable systems in ab initio studies of carbon nanosystems. The VSXC/STO-3G_{mag} calculated carbon chemical shifts in selected fullerenes (C_{60}, C_{70}, and C_{76}), used as relatively large objects for calculations predicted experimental values fairly accurately (RMS values from 1.5 to 3 ppm).

ASSOCIATED CONTENT

Supporting Information

Atom numbering in studied compounds, basis set dependence of structural parameters, IR/Raman vibrations and ^{13}C NMR shielding for benzene, phenol, aniline, and benzoic acid. Chemical shifts obtained with STO-3G_{mag} for model *zigzag* (4,0) SWCNT and C_{60}, C_{70}, and C_{76} fullerenes. This information is available free of charge via the Internet at http://pubs.acs.org/.

AUTHOR INFORMATION

Corresponding Author

*E-mail: teobaldk@gmail.com.

Notes

The authors declare no competing financial interest.

ACKNOWLEDGMENTS

This work was supported by the National Centre for Research and Development Grants PBS/A5/15/2012, GRAF-TECH/NCBR/10/29/2013 and partially by the Faculty of Chemistry, University of Opole (Grant 8/WCH/2012-S). Michał Stachów is a recipient of a Ph.D. fellowship from a project funded by the European Social Fund, ‚Uniwersytecki Program Stypendialny 2012−2013". The calculation facilities and software in the Supercomputing and Networking Center ACK CYFRONET AGH in Krakow within a calculation grant MNiSW/SGI3700/UOpolski/061/2012 and calculation facilities and software at the Supercomputing and Networking Center in Wrocław are also acknowledged. Magdalena Stobińska was supported by the Tekla Plus IV edition. The Grant Agency of the Czech Republic (P208/11/0105), the Academy of Sciences of the Czech Republic (M200551205) and the Ministry of Education, Youth and Sports (LH11033) of the Czech Republic are also acknowledged.

REFERENCES

(1) Radushkevich, L. V.; Lukyanovich, V. M. *J. Phys. Chem. (in Russian)* **1952**, *26*, 88−95.
(2) Iijima, S. *Nature* **1991**, *354*, 56−58.
(3) Iijima, A.; Ichihashi, T. *Nature* **1993**, *363*, 603−605.
(4) Kroto, H. W.; Heath, J. R.; O'Brien, S. C.; Curl, R. F.; Smalley, R. E. *Nature* **1985**, *318*, 162−163.
(5) Novoselov, K. S.; Geim, A. K.; Morozov, S. V.; Jiang, D.; Zhang, Y.; Dubonos, S. V.; Grigorieva, I. V.; Firsov, A. A. *Science* **2004**, *306*, 666−669.
(6) Saito, R.; Dresselhaus, M. S.; Dresselhaus, G. *Physical Properties of Carbon Nanotubes*; Imperial College Press: London, 1998.
(7) Thostenson, E. T.; Ren, Z.; Chou, T.-W. *Composite Sci. Technol.* **2001**, *61*, 1899−1912.
(8) Collins, P. G.; Avouris, P. *Sci. Am.* **2000**, *283*, 62−69.
(9) Ayala, P. Y.; Arenal, R.; Loiseau, A.; Rubio, A.; Pichler, T. *Rev. Mod. Phys.* **2010**, *82*, 1843−1885.
(10) Charlier, J.-C.; Blase, X.; Roche, S. *Rev. Mod. Phys.* **2007**, *79*, 677−732.
(11) Kummeth, F.; Ilani, S.; Ralph, D. C.; McEuen, P. L. *Nature* **2008**, *452*, 448−452.
(12) Braunecker, B.; Simon, P.; Loss, D. *Phys. Rev. Lett.* **2009**, *102*, 116403−116406.
(13) Churchill, H. O. H.; Bestwick, A. J.; Harlow, J. W.; Kuemmeth, F.; Marcos, D.; Stwertka, C. H.; Watson, S. K.; Marcus, C. M. *Nat. Phys.* **2009**, *5*, 321−326.
(14) Churchill, H. O. H.; Kuemmeth, F.; Harlow, J. W.; Bestwick, A. J.; Rashba, E. I.; Flensberg, K.; Stwertka, C. H.; Taychatanapat, T.; Watson, S. K.; Marcus, C. M. *Phys. Rev. Lett.* **2009**, *102*, 166802−166805.
(15) Abou-Rachid, H.; Hu, A.; Timoshevskii, V.; Song, Y.; Lussier, L.-S. *Phys. Rev. Lett.* **2008**, *100*, 196401−196404.
(16) Ebbesen, T. W.; Lezec, H. J.; Hiura, H.; Bennett, J. W.; Ghaemi, H. F.; Thio, T. *Nature*, *382*, 54-56.
(17) Peigney, A.; Laurent, C.; Flahaut, E.; Bacsa, R. R.; Rousset, A. *Carbon* **2001**, *39*, 507−514.
(18) Rzepka, M.; Lamp, P.; de la Casa-Lillo, M. A. *J. Phys. Chem. B* **1998**, *102*, 10894−10898.
(19) Schlapbach, L.; Züttel, A. *Nature* **2001**, *414*, 353−358.
(20) Nikitin, A.; Li, X.; Zhang, Z.; Ogasawara, H.; Dai, H.; Nilsson, A. *Nano Lett.* **2008**, *8*, 162−167.
(21) Kürti, J.; Kuzmany, H.; Burger, B.; Hulman, M.; Winter, J.; Kresse, G. *Synth. Met.* **1999**, *103*, 2508−2509.
(22) Kuzmany, H.; Plank, W.; Hulman, M.; Kramberger, C.; Gruneis, A.; Pichler, T.; Peterlik, H.; Kataura, H.; Achiba, Y. *Eur. Phys. J. B* **2001**, *22*, 307−320.
(23) Lolli, G.; Zhang, L.; Balzano, L.; Sakulchaicharoen, N.; Tan, Y.; Resasco, D. E. *J. Phys. Chem. B* **2006**, *110*, 2108−2115.

(24) Dresselhaus, M. S.; Dresselhaus, G.; Jorio, A. *J. Phys. Chem. C* **2007**, *111*, 17887−17893.
(25) Chang, T. *Acta. Mech. Sin.* **2007**, *23*, 159−162.
(26) Breitmaier, E.; Voelter, W. *Carbon-13 NMR Spectroscopy: High-Resolution Methods and Applications in Organic Chemistry and Biochemistry*; VCH: New York, 1987.
(27) Nagano, M.; Hasegawa, T.; Myoujin, N.; Yamaguchi, J.; Itaka, K.; Fukumoto, H.; Yamamoto, T.; Koinuma, H. *Jpn. J. Appl. Phys.. Part 2 Lett.* **2004**, *43*, L315−L316.
(28) Clewett, C. F. M.; Pietraß, T. *J. Phys. Chem. B* **2005**, *109*, 17907−17912.
(29) Proctor, W. G.; Yu, F. C. *Phys. Rev.* **1951**, *81*, 20−30.
(30) Pople, J. A.; Schneider, W. G.; Bernstein, H. J. *High-Resolution Nuclear Magnetic Resonance*; McGraw-Hill: New York, 1959.
(31) Ramsey, N. F. *Phys. Rev.* **1950**, *78*, 699−703.
(32) Engtrakul, C.; Davies, M. F.; Mistry, K.; Larsen, B. A.; Dillon, A. C.; Heben, M. J.; Blackburn, J. L. *J. Am. Chem. Soc.* **2010**, *132*, 9956−9957.
(33) Zurek, E.; Autschbach, J. *J. Am. Chem. Soc.* **2004**, *126*, 13079−13088.
(34) Zurek, E.; Pickard, C. J.; Walczak, B.; Autschbach, J. *J. Phys. Chem. A* **2006**, *110*, 11995−12004.
(35) Zurek, E.; Autschbach, J. *Int. J. Quant. Chem.* **2009**, *109*, 3343−3367.
(36) Kitaygorodskiy, A.; Wang, W.; Xie, X.-Y.; Lin, Y.-Y.; Shiral Fernando, K. A.; Wang, X.; Qu, L.; Chen, B.; Sun, Y.-P. *J. Am. Chem. Soc.* **2005**, *127*, 7517−7520.
(37) Tummala, N. R.; Morrow, B. H.; Resasco, D. E.; Striolo, A. *ACS Nano* **2010**, *4*, 7193−7204.
(38) Veloso, M. V.; Filho, A. G. S.; Filho, J. M.; Fagan, S. B.; Mota, R. *Chem. Phys. Lett.* **2006**, *430*, 71−74.
(39) Puzzarini, C.; Barone, V. *Int. J. Quant. Chem.* **2010**, *110*, 637−655.
(40) Parr, R. G.; Yang, W. *Density Theory of Atoms and Molecules*; Oxford University Press: New York, 1989.
(41) Errol, G. L. *Computational Chemistry: Introduction to the Theory and Applications of Molecular and Quantum Mechanics*; 2nd ed.; Springer: New York, 2010.
(42) Cizek, J. *J. Chem. Phys.* **1966**, *45*, 4256−4266.
(43) Raghavachari, K.; Trucks, G. W.; Pople, J. A.; Head-Gordon, M. *Chem. Phys. Lett.* **1989**, *157*, 479−483.
(44) Labanowski, J. K.; Anzelm, J. W. *Density Functional Methods in Chemistry*; Springer-Verlag: New York, 1991.
(45) Becke, A. D. *J. Chem. Phys.* **1993**, *98*, 5648−5652.
(46) Kohn, W.; Sham, L. J. *Phys. Rev.* **1965**, *140*, A1133−A1138.
(47) Kupka, T.; Stachów, M.; Nieradka, M.; Kaminský, J.; Pluta, T.; Sauer, S. P. A. *Magn. Reson. Chem.* **2011**, *49*, 231−236.
(48) Jensen, F. *Introduction to Computational Chemistry*; John Wiley and Sons: Chichester, England, 1999.
(49) Hehre, W. J.; Radom, L.; Schleyer, P. v. R.; Pople, J. A. *Ab Initio Molecular Orbital Theory*; Wiley: New York, 1986.
(50) Kupka, T.; Ruscic, B.; Botto, R. E. *J. Phys. Chem. A* **2002**, *106*, 10396−10407.
(51) Kupka, T.; Stachów, M.; Nieradka, M.; Kaminský, J.; Pluta, T. *J. Chem. Theor. Comput.* **2010**, *6*, 1580−1589.
(52) Kupka, T.; Nieradka, M.; Stachów, M.; Pluta, T.; Nowak, P.; Kjear, H.; Kongsted, J.; Kaminský, J. *J. Phys. Chem. A* **2012**, *116*, 3728−3738.
(53) Helgaker, T.; Klopper, W.; Koch, H.; Noga, J. *J. Chem. Phys.* **1997**, *106*, 9639−9646.
(54) Foresman, J. B.; Frisch, A. *Exploring Chemistry with Electronic Structure Methods*; 2nd ed.; Gaussian Inc: Pittsburg, PA, 1996.
(55) Feller, D.; Peterson, K. A. *J. Chem. Phys.* **1998**, *108*, 154−176.
(56) Feller, D. *J. Comput. Chem.* **1996**, *17*, 1571−1586.
(57) Broda, M. A.; Buczek, A.; Kupka, T.; Kaminský, J. *Vibr. Spectrosc.* **2012**, *63*, 432−439.
(58) Liu, L. V.; Tian, W. Q.; Chen, Y. K.; Zhang, Y. A.; Wang, Y. A. *Nanoscale* **2010**, *2*, 254−261.
(59) Chełmecka, E.; Pasterny, K.; Kupka, T.; Stobiński, L. *J. Mol. Model.* **2012**, *18*, 1463−1472.
(60) Chełmecka, E.; Pasterny, K.; Kupka, T.; Stobiński, L. *J. Mol. Struct. (Theochem)* **2010**, *948*, 93−98.
(61) Latil, S.; Henrard, L.; Goze Bac, C.; Bernier, P.; Rubio, A. *Phys. Rev. Lett.* **2001**, *86*, 3160−3163.
(62) Besley, N. A.; Titman, J. J.; Wright, M. D. *J. Am. Chem. Soc.* **2005**, *127*, 17948−17953.
(63) Mauri, F.; Pfrommer, B. G.; Louie, S. G. *Phys. Rev. Lett.* **1996**, *77*, 5300−5303.
(64) Marques, M. A. L.; d'Avezac, M.; Mauri, F. *Phys. Rev. B* **2006**, *73*, 125433−125439.
(65) Hayashi, S.; Hoshi, F.; Ishikura, T.; Yumura, M.; Ohshima, S. *Carbon* **2003**, *41*, 3047−3056.
(66) Kupka, T.; Stachów, M.; Nieradka, M.; Stobiński, L. *Magn. Reson. Chem.* **2011**, *49*, 549−557.
(67) Kupka, T.; Stachów, M.; Chełmecka, E.; Pasterny, K.; Stobiński, L. *Synth. Met.* **2012**, *162*, 573−583.
(68) Kupka, T.; Chełmecka, E.; Pasterny, K.; Stachów, M.; Stobiński, L. *Magn. Reson. Chem.* **2012**, *50*, 142−151.
(69) Jensen, F. *J. Chem. Theor. Comput.* **2008**, *4*, 719−727.
(70) Voronkov, E.; Rossikhin, V.; Okovytyy, S.; Shatckih, A.; Bolshakov, V.; Leszczynski, J. *Int. J. Quantum Chem.* **2012**, *112*, 2444−2449.
(71) Voronkov, E. O.; Kuz'menko, V. V.; Rossikhin, V. V. *Theor. Exp. Chem.* **1989**, *24*, 511−515.
(72) Voronkov, E. O.; Rossikhin, V. V. *Theor. Math. Phys.* **1981**, *48*, 647−652.
(73) Ditchfield, R. *Mol. Phys.* **1974**, *27*, 789−807.
(74) Wolinski, K.; Hinton, J. F.; Pulay, P. *J. Am. Chem. Soc.* **1990**, *112*, 8251−8260.
(75) Frisch, M. J.; Trucks, G. W.; Schlegel, H. B.; Scuseria, G. E.; Robb, M. A.; Cheeseman, J. R.; Scalmani, G.; Barone, V.; Mennucci, B.; Petersson, G. A.; Nakatsuji, H.; Caricato, M.; Li, X.; Hratchian, H. P.; Izmaylov, A. F.; Bloino, J.; Zheng, G.; Sonnenberg, J. L.; Hada, M.; Ehara, M.; Toyota, K.; Fukuda, R.; Hasegawa, J.; Ishida, M.; Nakajima, T.; Honda, Y.; Kitao, O.; Nakai, H.; Vreven, T.; J. A. Montgomery, J.; Peralta, J. E.; Ogliaro, F.; Bearpark, M.; Heyd, J. J.; Brothers, E.; Kudin, K. N.; Staroverov, V. N.; Kobayashi, R.; Normand, J.; Raghavachari, K.; Rendell, A.; Burant, J. C.; Iyengar, S. S.; Tomasi, J.; Cossi, M.; Rega, N.; Millam, J. M.; Klene, M.; Knox, J. E.; Cross, J. B.; Bakken, V.; Adamo, C.; Jaramillo, J.; Gomperts, R.; Stratmann, R. E.; Yazyev, O. ; Austin, A. J.; Cammi, R.; Pomelli, C.; Ochterski, J. W.; Martin, R. L.; Morokuma, K.; Zakrzewski, V. G.; Voth, G. A.; Salvador, P.; Dannenberg, J. J.; Dapprich, S.; Daniels, A. D.; Farkas, O.; Foresman, J. B.; Ortiz, J. V.; Cioslowski, J.; Fox, D. J. *Gaussian*; Gaussian, Inc.: Wallingford, CT, 2009.
(76) Lee, C.; Yang, W.; Parr, R. G. *Phys. Rev. B* **1988**, *37*, 785−789.
(77) Van Voorhis, T.; Scuseria, G. E. *J. Chem. Phys.* **1988**, *109*, 400−410.
(78) Gauss, J.; Stanton, J. F. *J. Phys. Chem. A* **2000**, *104*, 2865−2868.
(79) Goodman, L.; Ozkabak, A. G.; Thakur, S. N. *J. Phys. Chem.* **1991**, *95*, 9044−9058.
(80) Martin, J. L. M.; Taylor, P. R.; Lee, T. J. *Chem. Phys. Lett.* **1997**, *275*, 414−422.
(81) Berces, A.; Ziegler, T. *J. Chem. Phys.* **1993**, *98*, 4793−4804.
(82) Ohno, K.; Maeda, S. *Chem. Phys. Lett.* **2011**, *503*, 322−328.
(83) Larsen, N. W. *J. Mol. Struct.* **1979**, *51*, 175−190.
(84) Michalska, D.; Bieńko, D. C.; Abkowicz-Bieńko, A. J.; Latajka, Z. *J. Phys. Chem.* **1996**, *100*, 17786−17790.
(85) Keresztury, G.; Billes, F.; Kubinyi, M.; Sundius, T. *J. Phys. Chem. A* **1998**, *102*, 1371−1380.
(86) Giuliano, B. M.; Reva, I.; Lapinski, L.; Fausto, R. *J. Chem. Phys.* **2012**, *136*, 024505−024511.
(87) O'Malley, P. J. *J. Mol. Struct. (Theochem)* **2005**, *755*, 147−150.
(88) Michalska, D.; Zierkiewicz, W.; Bieńko, D. C.; Wojciechowski, W.; Zeegers-Huyskens, T. *J. Phys. Chem. A* **2001**, *105*, 8734−8739.
(89) Wojciechowski, P. M.; Zierkiewicz, W.; Michalska, D.; Hobza, P. *J. Chem. Phys.* **2003**, *118*, 10900−10911.

(90) Lister, D. G.; Tyler, J. K.; Hog, J. H.; Larsen, N. W. *J. Mol. Struct.* **1974**, *23*, 253−264.
(91) Gee, C.; Douin, S.; Crepin, C.; Brechignac, P. *Chem. Phys. Lett.* **2001**, *338*, 130−136.
(92) Evans, J. C. *Spectrochim. Acta* **1960**, *16*, 428−442.
(93) Aarset, K.; Page, E. M.; Rice, D. A. *J. Phys. Chem. A* **2006**, *110*, 9014−9019.
(94) Alcolea Palafox, M.; Nunez, J. L.; Gil, M. *Int. J. Quant. Chem.* **2002**, *89*, 1−24.
(95) Santos, L. M. N. B. F.; Rocha, M. A. A. *J. Chem. Eng. Data* **2010**, *55*, 2799−2808.
(96) Bakker, J. M.; Mac Aleese, L.; von Helden, G.; Meijer, G. *J. Chem. Phys.* **2003**, *119*, 11180−1185.
(97) Florio, G. M.; Zwier, T. S.; Myashakin, E. M.; Jordan, K. D.; Sibert, E. L., III *J. Chem. Phys.* **2003**, *118*, 1735−1746.
(98) Antony, J.; von Helden, G.; Meijer, G.; Schmidt, B. *J. Chem. Phys.* **2005**, *123*, 014305−014311.
(99) Reva, I. D.; Stepanian, S. G. *J. Mol. Struct.* **1995**, *349*, 337−340.
(100) Stepanian, S. G.; Reva, I. D.; Radchenko, E. D.; Sheina, G. G. *Vibr. Spectrosc.* **1996**, *11*, 123−133.
(101) Brock, C. P.; Dunitz, J. D.; Hirschfeld, F. L. *Acta Crystallogr., Sect. B: Struct. Sci.* **1991**, *47*, 789−797.
(102) Robertson, J. M.; Sinclair, V. C.; Trotter, J. *Acta Crystallogr.* **1961**, *14*, 697−704.
(103) Campbell, R. B.; Robertson, J. M.; Trotter, J. *Acta Crystallogr.* **1961**, *14*, 705−711.
(104) Dunning, T. H., Jr. *J. Phys. Chem. A* **2000**, *104*, 9062−9080.
(105) Jackowski, K.; Maciąga, E.; Wilczek, M. *J. Mol. Struct.* **2005**, *744*−*747*, 101−105.
(106) Katritzky, A. R. *Handbook of Heterocyclic Chemistry*; Pergamon Press: Oxford, 1985.
(107) Salsbury, F. R. J.; Harris, R. A. *Chem. Phys. Lett.* **1997**, *279*, 247−251.
(108) *Spectral Database for Organic Compounds, SDBS*; National Institute of Advanced Industrial Science and Technology (AIST): Japan; http://sdbs.riodb.aist.go.jp/sdbs/cgi-bin/cre_index.cgi?lang=eng.
(109) Houk, K. N.; Lee, P. S.; Nendel, M. *J. Org. Chem.* **2001**, *66*, 5517−5521.
(110) Wiberg, K. B. *J. Org. Chem.* **1997**, *62*, 5720−5727.
(111) Biermann, D.; Schmidt, W. *J. Am. Chem. Soc.* **1980**, *102*, 3163−3173.
(112) Lof, R. W.; Van Veenendaal, M. A.; Koopmans, B.; Jonkman, H. T.; Sawatzky, G. A. *Phys. Rev. Lett.* **1992**, *68*, 3924−3927.
(113) Norton, J. E.; Houk, K. N. *J. Am. Chem. Soc.* **2005**, *127*, 4162−4163.
(114) Kaur, I.; Jia, W.; Kopreski, R. P; Selvarasah, S.; Dokmeci, M. R; Pramanik, C.; McGruer, N. E; P., M. G. *J. Am. Chem. Soc.* **2008**, *130*, 16274−16286.
(115) Malloci, G.; Mulas, G.; Cappellini, G.; Joblin, C. *Chem. Phys.* **2007**, *340*, 43−58.
(116) Zade, S. S.; Bendikov, M. *Angew. Chem., Int. Ed.* **2010**, *49*, 4012−4015.
(117) Engtrakul, C.; Irurzun, V. M.; Gjersing, E. L.; Holt, J. M.; Larsen, B. A.; Resasco, D. E.; Blackburn, J. L. *J. Am. Chem. Soc.* **2012**, *134*, 4850−4856.
(118) Ci, L.; Zhou, Z.; Tang, D.; Yan, X.; Liang, Y.; Liu, D.; Yuan, H.; Zhou, W.; Wang, G.; Xie, S. *Chem. Vap. Deposition* **2003**, *9*, 119−121.
(119) Arnold, M. S.; Green, A. A.; Hulvat, J. F.; Stupp, S. I.; Hersam, M. C. *Nat. Nano* **2006**, *1*, 60−65.
(120) Kaminský, J.; Budesinský, M.; Taubert, S.; Bour, P.; Straka, M. *Phys. Chem. Chem. Phys.* **2013**, *15*, 9223−9230.